

## 6. Supplementary Material

### 6.1. Proof that Magnitude-Rewarding Functions Suffer Worse Aperture-Uncertainty

In Section 2.1 we discuss why magnitude-rewarding rewards are likely to fail on line features (due to aperture uncertainty), together with a visual example (Fig. 4) and plots of line features in real data (Fig. 6). Here we will prove this notion geometrically.

As a line feature moves across the image, it generates a plane of events. If one only considers event warp trajectories that run parallel to the plane, the possible trajectories become two-dimensional - we can thus model the event plane as a rectangle of height  $h$  and width  $w$  (see Fig. 13).

Computing the sum of event accumulations along the actual trajectory of the line feature then just becomes

$$\int_a^b h dx, \quad (9)$$

with the  $r_{\text{SoS}}$

$$r_{\text{SoS}} = \int_a^b h^2 dx. \quad (10)$$

Likewise, incorrect projections parallel to the plane of events can now be modeled by rotations of the rectangle around point  $b$  by some angle  $\phi$  (see Fig. 14), where essentially we rotate the events instead of rotating the warp vector.

The accumulation of events can now be written as a piecewise function over the regions  $A, B, C$ , which are bounded by the lines  $f_1(x), f_2(x), f_3(x)$  and  $f_4(x)$ . If  $\mathbf{I}$  is set to equal  $(0, 0)$ , then

$$\text{I} = (0, 0) \quad (11)$$

$$\text{II} = (-w \cos(\phi), w \cos(\phi)) \quad (12)$$

$$\text{III} = (-w \cos(\phi) + h \sin(\phi), w \cos(\phi) + h \cos(\phi)) \quad (13)$$

$$\text{IV} = (h \sin(\phi), h \cos(\phi)). \quad (14)$$

Thus,

$$f_1(x) = -\tan(\phi)x \quad (15)$$

$$f_2(x) = x \cot(\phi) + w \csc(\phi) \quad (16)$$

$$f_3(x) = h \sec(\phi) - x \tan(\phi) \quad (17)$$

$$f_4(x) = \cot(\phi)x \quad (18)$$

The function for the sum of accumulations can now be written as the piecewise function

$$f_{\text{sum}}(x) = \begin{cases} \begin{cases} \csc(\phi)(w + x \sec(\phi)) & a \leq x < d \\ h \sec(\phi) & d \leq x < b \end{cases} & b > d \\ \begin{cases} \sec(\phi)(h - x \csc(\phi)) & b \leq x < c \\ \csc(\phi)(w + x \sec(\phi)) & a \leq x < b \\ w \csc(\phi) & b \leq x < d \\ \sec(\phi)(h - x \csc(\phi)) & d \leq x < c \end{cases} & b \leq d \end{cases} \quad (19)$$

The double piecewise function is necessary, since there are two distinct cases as  $\phi$  increases (see Fig. 15); that when  $b > d$  and that when  $b \leq d$ .

The integral of  $f_{\text{sum}}(x)$  is

$$\int_a^c f_{\text{sum}}(x) = \begin{cases} h^2 \tan(\phi) + h(w - h \tan(\phi)) & b > d \\ w^2 \cot(\phi) + w(h - w \cot(\phi)) & b \leq d, \end{cases} \quad (20)$$

which after a bit of rearranging comes out as

$$\int_a^c f_{\text{sum}}(x) = \begin{cases} hw & b > d \\ hw & b \leq d, \end{cases} \quad (21)$$

(as one would expect, since the area of the original rectangle is invariant). If we now however look as the  $r_{\text{SoS}}$  of the rotated rectangle, things are a little more interesting. To get this, we simply integrate the square of  $f_{\text{sum}}(x)$ :

$$f_{\text{sum}}(x)^2 = \begin{cases} \begin{cases} \csc(\phi)^2(w + x \sec(\phi))^2 & a \leq x < d \\ h^2 \sec(\phi)^2 & d \leq x < b \end{cases} & b > d \\ \begin{cases} \sec(\phi)^2(h - x \csc(\phi))^2 & b \leq x < c \\ \csc(\phi)^2(w + x \sec(\phi))^2 & a \leq x < b \\ w^2 \csc(\phi)^2 & b \leq x < d \\ \sec(\phi)^2(h - x \csc(\phi))^2 & d \leq x < c \end{cases} & b \leq d \end{cases} \quad (22)$$

and

$$\int_a^c f_{\text{sum}}(x)^2 = \begin{cases} \frac{2}{3} h^3 \tan(\phi) \sec(\phi) + \sec(\phi) h^2 w & b > d \\ \frac{2}{3} w^3 \cot(\phi) \csc(\phi) + \csc(\phi) w^2 h & b \leq d \end{cases} \quad (23)$$

$$= r_{\text{SoS}} \quad (24)$$

This integral is the familiar  $r_{\text{SoS}}$ . If we plot (23) for  $0 \leq \phi \leq \pi/2$ ,  $w = 10$  and a range of values for  $h$  (see Fig. 16), we see that the actual maximum of the  $r_{\text{SoS}}$  is only at  $\phi = 0$  (as it should be), when  $h \gg w$ .

In the case of events, the ‘‘height’’ of the event plane is only much greater than the width when a lot of time passes, since the time axis is the equivalent of  $h$  in this analogy. This shows rather neatly, not only why magnitude-rewarding rewards fail with line features, but that this uncertainty is dependent on the accumulation time.

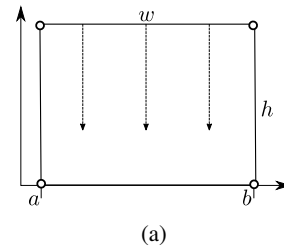


Figure 13: The event plane represented as a rectangle; the actual trajectory of the line feature is shown as the dashed arrows.

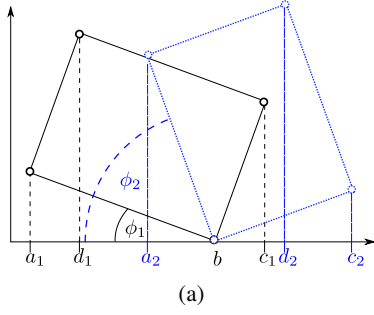


Figure 15: Two situations exist for  $0 \leq \phi \leq \pi/2$ : that  $d \leq b$  (black) and  $b \leq d$  (blue)

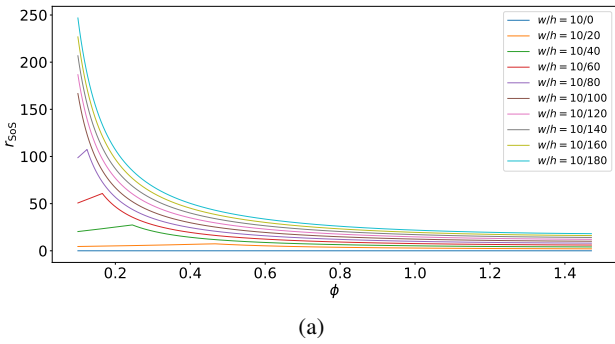


Figure 16: Plot of the  $r_{SoS}$  for various ratios of  $w/h$ , over  $0 \leq \phi \leq \pi/2$ .

We can show this formally too; looking at the equations

$$\frac{2}{3}h^3 \tan(\phi) \sec(\phi) + \sec(\phi)h^2w \quad (25)$$

$$\frac{2}{3}w^3 \cot(\phi) \csc(\phi) + \csc(\phi)w^2h \quad (26)$$

from (23), note that (25) is monotonically increasing for all values of  $0 \leq \phi \leq \pi/2$  in the range  $b > d$  and that (26) is monotonically decreasing for all values of  $0 \leq \phi \leq \pi/2$  in the range  $b \leq d$  (for fixed values of  $w$  and  $h$ , a valid assumption since the dimensions of the event plane don't change). This means that the maximum of the total function (23) is at the point where (25) = (26). Then

$$\frac{h^2}{w^2} = \cot^2(\phi) \quad (27)$$

and

$$\phi = \cot^{-1} \sqrt{\frac{h^2}{w^2}}. \quad (28)$$

Solving for  $\phi = 0$ ,

$$0 = \cot^{-1} \sqrt{\frac{h^2}{w^2}} \quad (29)$$

for which no solution exists. However,

$$\lim_{n \rightarrow \infty} \cot^{-1} \sqrt{x} = 0. \quad (30)$$

Therefore the ratio of  $\frac{h}{w}$  must be very large in order to get the correct trajectory of a line feature using magnitude-rewarding rewards.

The analogy for sparsity-rewarding rewards such as the  $r_{SoSA}$  is of course the length of the range  $[a, c]$ , since this corresponds to the count of locations to which events have projected. The equation describing this measure is

$$\frac{1}{a-b} = \frac{1}{h \sin(\phi) + w \cos(\phi)} \quad (31)$$

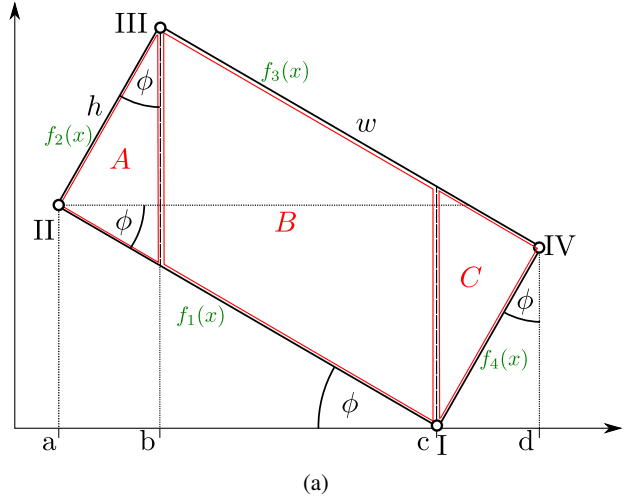


Figure 14: The event plane represented as a rectangle; different trajectories (parallel to the event plane) are represented by rotations of the rectangle around point  $b$  by rotation  $\phi$ .

This is a convex function on the range  $0 \leq \phi \leq \pi/2$ , therefore the maximum must lie at either 0 or  $\pi/2$  on  $0 \leq \phi \leq \pi/2$  So the problem becomes, for which  $w, h$  is

$$\frac{1}{h \sin(0) + w \cos(0)} > \frac{1}{h \sin(\pi/2) + w \cos(\pi/2)} \quad (32)$$

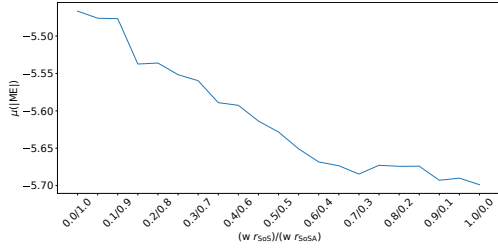
$$= \frac{1}{w} > \frac{1}{h} \quad (33)$$

$$= h > w \quad (34)$$

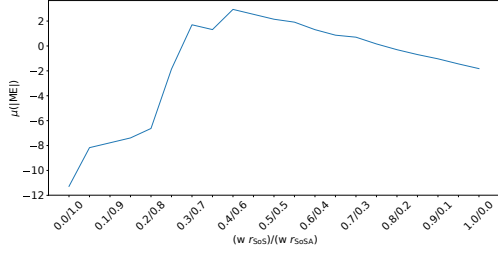
For a visualization of this, see the plots in Fig. 17. And with that we have proven that optimizing contrast with sparsity-rewarding functions can allow convergence to the true trajectory of pure line segments, whereas magnitude rewarding functions cannot.

## 6.2. Weighted Sums

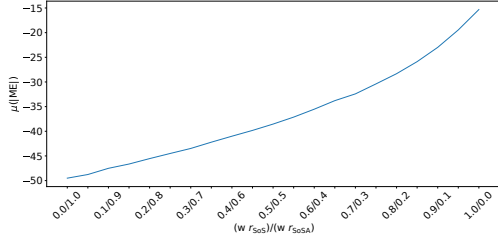
Since the errors presented in Section 4 had different standard deviations, we thought it would be worth looking at how weighted combinations of magnitude- and sparsity-rewarding function perform. To this end we present the following plots in Fig. 18. To generate these we estimated the optic flow of the office sequence (see Section 4.3) various times using different weighted combinations of the  $r_{SoS}$  and  $r_{SoSA}$ . The plots indicate that with no noise it



(a) Error for weighted sum for event/noise ratio 1/0 (no noise).



(b) Error for weighted sum for event/noise ratio 1/2.



(c) Error for weighted sum for event/noise ratio 1/10.

Figure 18: Plots for the error of the estimates vs the sum weights for weighted sums of  $r_{\text{SoS}}$  and  $r_{\text{ISoA}}$  at different event to noise ratios.

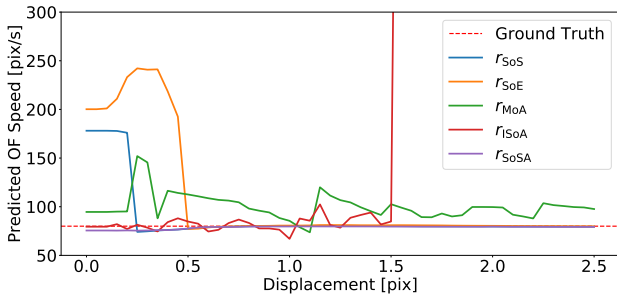
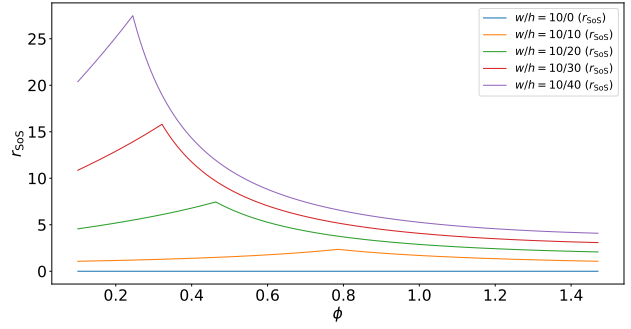
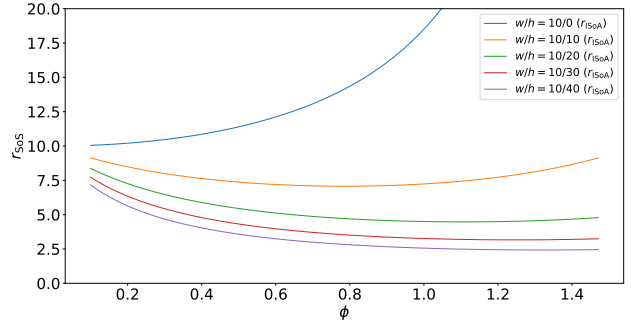


Figure 19: Plot for the velocity estimates of various rewards for various values of  $\sigma$ .



(a) Plot of the  $r_{\text{SoS}}$  for various ratios of  $w/h$ , over  $0 \leq \phi \leq \pi/2$ .



(b) Plot of the  $r_{\text{ISoA}}$  for various ratios of  $w/h$ , over  $0 \leq \phi \leq \pi/2$

Figure 17: Comparison of theoretical convergence behavior of  $r_{\text{SoS}}$  vs  $r_{\text{ISoA}}$ .

is better to use only  $r_{\text{SoSA}}$  and if there is some to use a combination. If there is a lot of noise it is better to use  $r_{\text{SoS}}$ . This supports the conclusions drawn in the rest of the paper. Note that the  $r_{\text{R1}}$  and  $r_{\text{R2}}$  reward are still better than these linear combinations.

### 6.3. Blurring $\sigma$

In practice, convergence in optimizing the contrast is greatly aided by applying a blurring kernel to the image of warped events. In this experiment we aim to discover which value of  $\sigma$  is best for which reward. To do this we estimated optical flow on the circle sequence (Section 4.2) using various blur sigmas. As can be seen, the different rewards have quite different reactions to different degrees of blurring. However, a value of  $\sigma = 1$  seems to give reasonable results across all of the rewards and is the value we used in other experiments.